Linshan Shang,[1] Haiqing Hua,[1,2] Kylie Foo,[2] Hector Martinez,[1] Kazuhisa Watanabe,[2] Matthew Zimmer,[1] David J. Kahler,[1] Matthew Freeby,[2] Wendy Chung,[2] Charles LeDuc,[2] Robin Goland,[2] Rudolph L. Leibel,[2] and Dieter Egli[1]

β-Cell Dysfunction Due to Increased ER Stress in a Stem Cell Model of Wolfram Syndrome

Wolfram syndrome is an autosomal recessive disorder caused by mutations in *WFS1* and is characterized by insulin-dependent diabetes mellitus, optic atrophy, and deafness. To investigate the cause of β-cell failure, we used induced pluripotent stem cells to create insulin-producing cells from individuals with Wolfram syndrome. WFS1-deficient β-cells showed increased levels of endoplasmic reticulum (ER) stress molecules and decreased insulin content. Upon exposure to experimental ER stress, Wolfram β-cells showed impaired insulin processing and failed to increase insulin secretion in response to glucose and other secretagogues. Importantly, 4-phenyl butyric acid, a chemical protein folding and trafficking chaperone, restored normal insulin synthesis and the ability to upregulate insulin secretion. These studies show that ER stress plays a central role in β-cell failure in Wolfram syndrome and indicate that chemical chaperones might have therapeutic relevance under conditions of ER stress in Wolfram syndrome and other forms of diabetes.

Diabetes 2014;63:923–933 | DOI: 10.2337/db13-0717

All forms of diabetes are ultimately the result of an inability of pancreatic β-cells to provide sufficient insulin in response to ambient blood glucose concentrations. Stem cell–based models of diabetes should enable analysis of specific pathways leading to human β-cell failure and the testing of strategies to preserve or restore β-cell function.

Childhood-onset insulin-dependent diabetes can be caused by mutations in *WFS1* gene (wolframin), which is highly expressed in human islets as well as in the heart, brain, placenta, and lung (1). Wolfram syndrome subjects are also affected by optic atrophy, deafness, ataxia, dementia, and psychiatric illnesses (2). The disease is fatal, and no treatments for the diabetes other than provision of exogenous insulin are available. Postmortem analyses of pancreata of Wolfram patients show a selective loss of pancreatic β-cells (3). In the mouse, loss of the *WFS1* gene results in impaired glucose-stimulated insulin secretion and a reduction of β-cells in pancreatic islets (4,5). But unlike human subjects, these mice develop only mild or no diabetes (4). Several molecular mechanisms by which WFS1 deficiency might affect β-cell function have been described. WFS1 deficiency reduces insulin processing and acidification in insulin granules of mouse β-cells, where low pH is necessary for optimal insulin processing and granule exocytosis (6). In human fibroblasts, WFS1 localizes to the endoplasmic reticulum (ER) (7), where it increases free Ca^{2+} (8) and interacts with calmodulin in a Ca^{2+}-dependent manner (9). In mouse islets, following stimulation with glucose, WFS1 is found on the plasma membrane, where it appears to stimulate

[1]The New York Stem Cell Foundation Research Institute, New York, NY
[2]Division of Molecular Genetics, Department of Pediatrics and Naomi Berrie Diabetes Center, Columbia University, New York, NY

Corresponding author: Dieter Egli, d.egli@nyscf.org.

Received 3 May 2013 and accepted 6 November 2013.

This article contains Supplementary Data online at http://diabetes.diabetesjournals.org/lookup/suppl/doi:10.2337/db13-0717/-/DC1.

See accompanying article, p. 844.

cAMP synthesis through an interaction with adenylyl cyclase, thereby promoting insulin secretion (10). In addition, WFS1 deficiency is accompanied by activation of components of the unfolded protein response (UPR), such as GRP78 (78 kDa glucose-regulated protein)/Bip (Ig-binding protein) and XBP-1 (X-box-binding protein-1) and reduced ubiquitination of ATF6α (activating transcription factor-6α) (11,12). Because the relevance of these molecular mechanisms to β-cell dysfunction is unclear, and because of phenotypic differences between mice and human subjects, there is a need for a biological model of the consequences of WFS1 deficiency in the human β-cells.

We generated insulin-producing cells from skin fibroblasts of patients with Wolfram syndrome and found that these *WFS1* mutant cells display insulin processing and secretion in response to various secretagogues comparable to healthy controls but have a lower insulin content and increased activity of UPR pathways. The chemical chaperone, 4-phenyl butyric acid (4PBA), reduced the activity of UPR pathways and restored insulin content to levels comparable to controls. Experimental ER stress induced by exposure to low concentrations of thapsigargin (TG), impaired insulin processing, and abolished insulin secretion in response to various secretagogues, while β-cell function in control cells was unaffected. Importantly, genetic rescue of *WFS1* restored insulin content and preserved the ability to secrete insulin under conditions of ER stress. These results demonstrate that ER stress plays a central role in β-cell dysfunction in Wolfram syndrome and identify a potential approach to clinical intervention.

RESEARCH DESIGN AND METHODS

Research Subjects and Generation of Induced Pluripotent Stem Cells

Skin biopsies were obtained from subjects WS-1 (biopsy 1–088) and WS-2 (biopsy 1–071) at the Naomi Berrie Diabetes Center using a 3 mm AcuPunch biopsy kit (Acuderm Inc.). Skin fibroblasts were derived and grown as previously described. Fibroblast cells from WS-3, WS-4, and *WFS1* mutation carrier were obtained from Coriell Research Institute. Induced pluripotent stem (iPS) cells were generated using the CytoTune-iPS Sendai Reprogramming Kit (Invitrogen) (13) or using retroviral vectors (14). To genetically rescue the *WFS1* locus, Wolfram iPS cell lines were transfected with lentivirus containing wild-type *WFS1* cDNA sequence (from Addgene plasmid 13011) under murine stem cell virus promoter. Cell lines with stable integration were selected and maintained by puromycin treatment.

β-Cell Differentiation and Analysis

Human embryonic stem (ES) or iPS cells were dissociated by dispase (3–5 min) and Accutase (5 min; Sigma). Cells were suspended in human ES medium containing 10 μmol/L Y27632, a rho-associated protein kinase inhibitor, and filtered through a 70 μm cell strainer. Then cells were seeded at a density of 800,000 cells/well in 12-well plates. After 1 or 2 days, when cells reached 80–90% confluence, differentiation was performed as previously described (15). To quantify the number of insulin-positive cells within β-cell cultures, and to simultaneously quantify insulin and proinsulin content within β-cells, cells were dissociated to single cells and divided into three fractions: 20% of cells for quantification of positively stained cells using a Celigo Cytometer system (Cyntellect), 40% for RNA analysis, and 40% for ELISA assay to determine insulin content. For insulin content analysis, cells were lysed by M-PER protein extraction reagent (Thermo Scientific). Proinsulin and insulin content was measured with human proinsulin and insulin ELISA kits (Mercodia). To determine insulin and glucagon secretion in live cultures, β-cells were washed for 1 h in CMRL medium then incubated in CMRL medium containing 5.6 mmol/L glucose for 1 h, and the medium was collected. After that, CMRL medium containing 16.9 mmol/L glucose, 15 mmol/L arginine, 30 mmol/L potassium, 1 μmol/L Bay K8644, or 1 mmol/L dibutyl cAMP (DBcAMP) + 16.9 mmol/L glucose was added to the wells for 1 h, and the medium was collected. Human C-peptide concentration was measured by ultrasensitive human C-peptide ELISA kit (Mercodia), which specifically detects C-peptide, but not insulin or proinsulin. Glucagon levels in medium were measured with a glucagon ELISA kit (ALPCO Diagnostics).

UPR Analysis

iPS cells, fibroblasts, or β-cells were incubated for the indicated time and concentration of TG, tunicamycin (TM; Sigma), sodium 4PBA, or tauroursodeoxycholate (TUDCA; both from EMD Chemicals Inc.) was added 1 h prior to and during TG or TM treatment. For long-term 4PBA treatment, cells were incubated with 1 mmol/L 4PBA from day 9 to day 15 of differentiation. Primers for PCR analysis of XBP-1 gel-imaging (16), sXBP-1 for quantitative PCR (17), ATF4 (18), GRP78, and insulin are listed in Supplementary Table 1.

Gene and Protein Expression Analysis

RNA was isolated using RNAeasy plus kit (Qiagen). cDNA was generated by using a reverse transcriptase kit (Promega). Cells were lysed by using M-PER mammalian protein extraction reagent and NE-PER Nuclear and Cytoplasmic Extraction Kit (Thermo Scientific). Protein levels were determined by Western blot using the antibodies as listed: rabbit anti-ATF6α (ab37149, Abcam), rabbit anti-phospho-eIF2α (3597; Cell Signaling Technology), mouse anti-eIF2α (2103; Cell Signaling Technology), and mouse-anti-GRP78 antibody (sc-166490; Santa Cruz Biotechnology).

Electron Microscopic Analysis

For electron microscopic analysis, differentiated β-cells were fixed in 2.5% glutaraldehyde in 0.1 mol/L Sorenson's buffer (pH 7.2) for 1 h. Samples were processed and

imaged by the Diagnostic Service, Department of Pathology and Cell Biology, Columbia University. Secretory granule structure and ER morphology were visually recognized. The number of granules per cell was determined using ImageJ software.

Transplantation and Glucose-Stimulated Insulin Secretion Assay

At 12 days of differentiation, 2–3 million cells were detached using TrypLE (Invitrogen), pelleted, and mixed with 10–15 μl matrigel (BD Biosciences) before being transplanted into a kidney capsule of a NOD.Cg-*Prkdc*^{scid} *Il2rg*^{tm1Wjl}/*SzJ* (NSG) mouse (stock number 005557; The Jackson Laboratory), using methods as previously described for the transplantation of islets (19). Glucose stimulation assay was performed 3 months after transplantation. Mice were deprived of food overnight (12–14 h); water was available ad libitum. Each mouse was injected intraperitoneally with a glucose solution (1 mg/g body weight). Before and half an hour after glucose injection, capillary blood glucose was measured and venous blood samples were collected from the tail and submandibular vein. Human C-peptide concentration in the mouse serum was measured by using an ultrasensitive human C-peptide ELISA kit (Mercodia). Nephrectomy was performed on some mice after human C-peptide was detected in the mouse serum. For ER stress studies, TG was administrated by one dose injection of 1 mg/kg of TG intraperitoneally.

Statistical Analysis

One-way ANOVA was applied for multicomparison among groups. Student *t*-test (two-tailed) was used to compare pairs of experiments. $P_{\alpha} < 0.05$ was considered statistically significant.

Study Approval

Protocols to obtain skin biopsies were approved by the Columbia Institutional Review Board and Embryonic Stem Cell Research Oversight Committees. Human subjects gave signed informed consent. Animal protocols were approved by the Columbia Institutional Animal Care and Use Committee.

RESULTS

Wolfram iPS Cells Differentiate Into β-Cells

We obtained skin biopsies and established skin cell lines from two subjects with Wolfram syndrome designated WS-1 and WS-2. Sequencing of the *WFS1* locus revealed that WS-2 is homozygous for a frameshift mutation 1230–1233delCTCT (V412fsX440) and that WS-1 is compound heterozygous for V412fsX440 and missense mutation P724L, both mutations that had previously been reported in Wolfram subjects (1,20). Three additional skin cell lines were obtained from Coriell Research Institute from two siblings with Wolfram syndrome: WS-3 and WS-4 and an unaffected parent (carrier). Both WS-3 and WS-4 are compound heterozygous for the mutations W648X and G695V in the WFS1 protein (1) (Fig. 1*A*). All Wolfram subjects had childhood-onset diabetes, with the earliest onset at age 2 years for WS-2 and between ages 11 and 13 years for WS-1, WS-3, and WS-4. The relationship of these specific mutations to age of onset of diabetes is unknown. All subjects required treatment with exogenous insulin and had optic atrophy. WS-1 has no history of hearing loss or diabetes insipidus, but optic atrophy was discovered at age 14 years. For WS-2, diabetes insipidus and optic atrophy developed at age 13 years. Progressive visual loss and cognitive disabilities have developed in both WS-1 and WS-2. An ES cell line

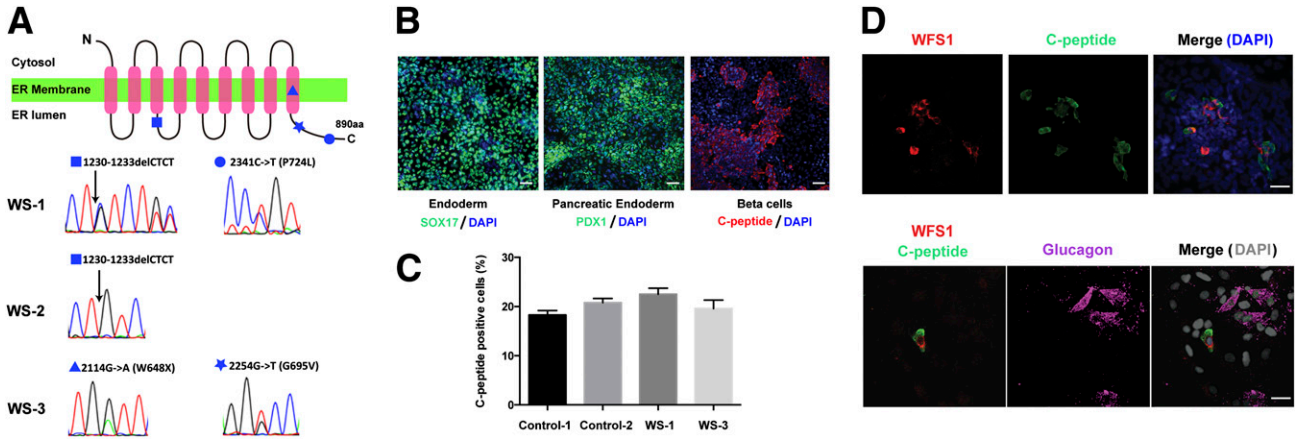

Figure 1—iPS cells from Wolfram subjects differentiated into insulin-producing cells. (*A*) Diagram of WFS1 structure showing the mutation sites and Sanger sequencing profiles in the four Wolfram subjects described here. Arrows indicate the four deleted nucleotides (CTCT). (*B*) Immunostaining of Wolfram cultures differentiated into endoderm (SOX17), pancreatic endoderm (PDX1), and C-peptide–positive cells. Scale bar, 50 μm. (*C*) Differentiation efficiency in controls and *WFS1* mutant cells determined by imaging (n = 10 for each of three independent experiments). (*D*) Immunostaining of WFS1, glucagon, and C-peptide in iPS-derived pancreatic cell cultures at d15 of differentiation. Scale bar, 20 μm.

HUES42 (21) (control-1) and an iPS cell line (control-2) generated from a healthy individual were used as normal controls. DNA sequencing confirmed that these two control cell lines do not carry any coding mutations in *WFS1*. To control for effects of genetic background, we included cells of the nondiabetic parent heterozygous for the mutation G695V in our analyses (Supplementary Table 1) and genetically rescued the *WFS1* locus by expressing a cDNA transgene under the murine stem cell virus promoter.

We generated iPS lines from the four Wolfram subjects and the control subjects using nonintegrating Sendai virus vectors encoding the transcription factors Oct4, Sox2, Klf4, and c-Myc (13). All iPS cell lines were karyotypically normal, expressed markers of pluripotency and differentiated into cell types and tissues of all three germ layers in vitro and after injection into immune-compromised mice (Supplementary Fig. 1). iPS cell lines from Wolfram and control subjects were differentiated into insulin-producing cells using stepwise differentiation into definitive endoderm (SOX17-positive cells), pancreatic endoderm (PDX1-positive cells), and β-cells (C-peptide-positive) (Fig. 1*B*). Differentiation efficiency of Wolfram cells was similar to controls: after 8 days of differentiation, approximately 80% of all cells expressed PDX1, a marker of pancreatic endocrine progenitors, and after 13 days of differentiation, approximately 20% of all cells expressed C-peptide (Fig. 1*C*, Supplementary Fig. 2). Immunostaining revealed that WFS1 was specifically expressed in insulin-producing cells but not in glucagon-positive cells (Fig. 1*D*), which is consistent with the expression pattern reported for mouse islets (5).

Activated UPR Reduces Insulin Synthesis in Wolfram β-Cells

To investigate the effects of *WFS1* mutations on β-cell function, we quantified insulin mRNA and protein content in Wolfram and control stem cell–derived β-cells. WFS1 deficiency was associated with a 40–50% reduction in insulin mRNA levels compared with controls (Fig. 2*A*), a 30–40% decrease of insulin protein content (Fig. 2*B*), and a 30–40% decrease in the number of secretory granules (Fig. 2*C* and *D*). Insulin production was restored to levels of control cells by a transgene encoding wild-type WFS1, indicating that WFS1 deficiency, and not other genetic differences, resulted in reduced insulin content (Fig. 2*A*–*D*).

To determine the cause of the decreased insulin content, we analyzed the ratio of proinsulin/insulin in β-cells. We found that the proinsulin/insulin ratio in Wolfram β-cells was between 0.4 and 0.55, similar to control cells (0.4–0.47) (Fig. 3*A*, Supplementary Fig. 3). We next investigated the expression of components of the UPR in Wolfram and control cells. Three branches of the UPR, inositol-requiring protein 1α (IRE1α), protein kinase RNA-like ER kinase (PERK), and ATF6, sense increases in unfolded protein and respond with modulation of cellular, transcriptional, and translational activities (22). It has previously been reported that chronic hyperactivation of IRE1 leads to decreased insulin mRNA and protein level in INS-1 cells (23). Using quantitative PCR and Western blotting, we found that in fibroblasts, iPS cells, and β-cells, components of the three major UPR pathways were increased in Wolfram subject samples in comparison with controls, including spliced XBP-1 (sXBP-1) mRNA, which is downstream of IRE1, ATF4 mRNA, and nuclear ATF6α, p-eIF2α (eukaryotic translation initiation factor-2α) and GRP78 protein (Fig. 3*B*–*E*, Supplementary Fig. 4). These differences were amplified by the imposition of experimental ER stress. TG, which impairs protein folding by interfering with calcium homeostasis in the ER (24), caused a greater increase of GRP78 mRNA levels in Wolfram (fourfold) than in control stem cells (twofold) (Supplementary Fig. 4*A*). A stronger UPR response in Wolfram cells than in control cells is also observed with the application of another ER stress inducer, TM, an inhibitor of *N*-linked glycosylation (25) (Supplementary Fig. 4*B* and *C*). Experimentally induced ER stress also affected ER morphology: the ER was greatly dilated in Wolfram β-cells in the presence of a low dose of TG, while control cells were unaffected (Fig. 3*G*, Supplementary Fig. 5). Insulin processing was similarly affected; treatment with low doses of TG resulted in the accumulation of proinsulin in Wolfram but not in control cells (Fig. 3*A*). The upregulation of UPR pathways, including increased sXBP-1 mRNA, a downstream target of IRE-1α, suggests that the UPR response is likely responsible for the reduced insulin content and insulin processing in β-cells.

To determine if preventing the activation of the UPR could restore normal insulin content in Wolfram cells, we generated β-cells in the presence of the chemical chaperone sodium 4PBA during days 9 to 15 of differentiation. 4PBA can assist protein folding and thereby reduce the activity of UPR pathways (26). 4PBA (27,28) and TUDCA (29) reduced GRP78 mRNA levels in Wolfram cells treated with TG (Fig. 3*F*). Nuclear ATF6α, p-eIF2α protein levels, and sXBP-1 as well as ATF4 mRNA levels were reduced by 30–50% in comparison with no 4PBA vehicle controls (Fig. 3*B*–*E*). Strikingly, insulin mRNA levels in Wolfram cells were increased by 1.9-fold and insulin content by 1.5–1.9-fold to levels comparable to those in control cells without 4PBA (Fig. 2*A* and *B*). The number of secretory granules in Wolfram β-cells was also substantially increased with the treatment of long-term 4PBA or with the expression of exogenous wild-type WFS1 protein (Fig. 2*C* and *D*). When control cells were exposed to the same 7d treatment with 4PBA during β-cell differentiation, no significant increase of insulin production was observed (Fig. 2*A* and *B*). Also, insulin processing was normalized by the treatment of 4PBA after exposure to TG (Fig. 3*A*). These results demonstrate that activation of the UPR mediates the reduced insulin content in *WFS1* mutant β-cells. The activation of all

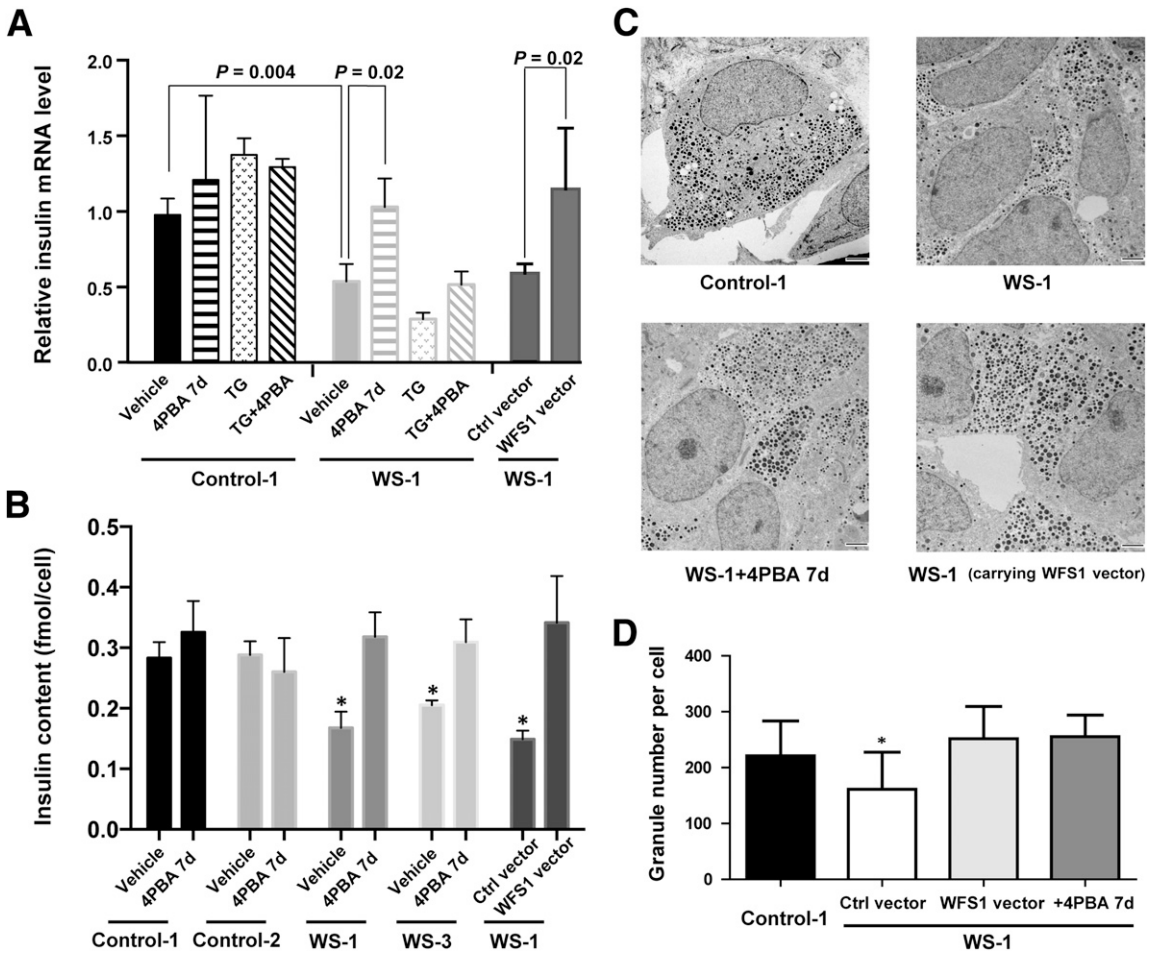

Figure 2—UPR-dependent reduction of insulin content in Wolfram β-cells. (*A*) Insulin mRNA levels in control and Wolfram β-cells normalized to TBP (TATA-binding protein) mRNA levels and to the number of C-peptide–positive cells used for analysis. (*B*) Insulin protein content in the β-cells normalized to the number of C-peptide–positive cells. Error bars represent three independent experiments with three replicates in each experiment. *$P < 0.05$ for vehicle of WS vs. control cells. (*C*) Transmission electron microscope images of β-cells (scale bar, 2 μm). (*D*) Quantification of granule numbers per cell. Three independent differentiation experiments with $n = 20$ sections for each subject of each experiment. *$P < 0.05$ for WS-1 vs. control or WS-1 cells treated with 4PBA for 7 days or WS-1 cells carrying wild-type *WFS1* expression vector. Ctrl, control.

three UPR pathways suggests that WFS1 acts upstream of the UPR, likely to maintain ER function under protein folding stress.

ER Stress Affects Stimulated Insulin Secretion in *WFS1* Mutant β-Cells

To determine whether a specific insulin secretion pathway was affected in Wolfram cells, we exposed them to various insulin secretagogues, including glucose, arginine, potassium, and the cAMP analog, DBcAMP. Others have previously reported that glucose stimulates insulin secretion by ATP generation, resulting in the closing of ATP-sensitive potassium channels and reduction of potassium efflux, which depolarizes the cell, stimulating Ca^{2+} influx and exocytosis of insulin granules (30). Arginine induces insulin secretion by triggering Ca^{2+} influx, without reducing potassium efflux (31). cAMP influences insulin secretion through activation of protein kinase A and/or exchange proteins activated by cAMP (32). Finally, extracellular potassium directly depolarizes the plasma membrane, resulting in the release of insulin granules (33). To assess insulin secretion in response to glucose, we incubated cells in 5.6 mmol/L glucose for 1 h, followed by incubation in 16.9 mmol/L glucose for 1 h. Control and the *WFS1* mutation carrier β-cells showed a 1.6- to 1.7-fold increase in C-peptide release in 16.9 mmol/L glucose (vs. 5.6 mmol/L glucose). A similar 1.5- to 1.9-fold increase was seen in the four *WFS1* mutant cell lines (Fig. 4*A* and *B*). Similarly, arginine, potassium, and DBcAMP increased C-peptide secretion (twofold to fourfold) equally in control and *WFS1* mutant cells (Fig. 4*A*). Therefore, *WFS1* mutant β-cells displayed functional responses to secretagogues acting at different points in pathways of metabolic sensing and insulin release comparable to control cells.

We next determined whether WFS1 deficiency affected stimulated insulin secretion under imposed ER

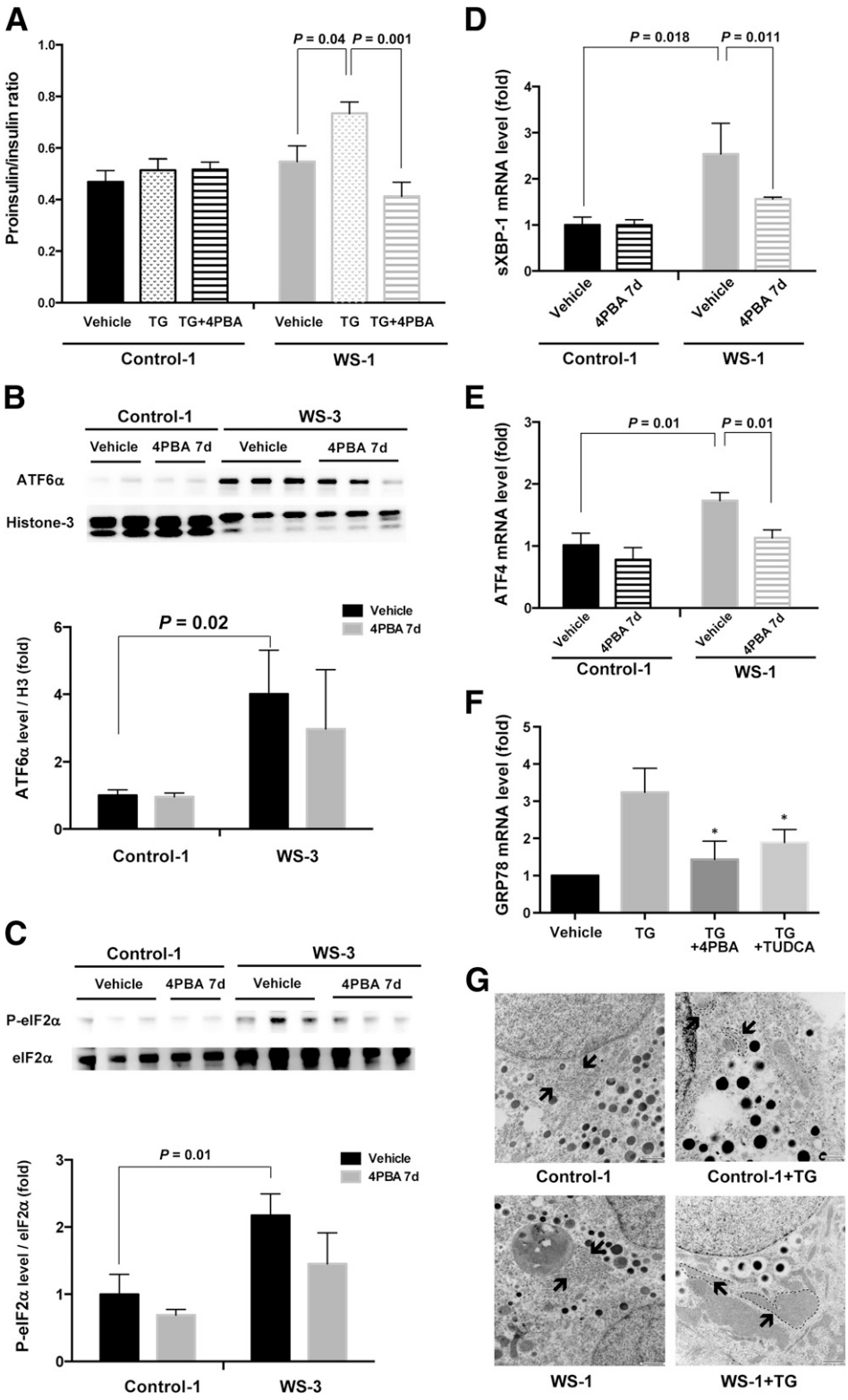

Figure 3—Increased UPR pathway activity and increased sensitivity of the ER-to-ER stress in Wolfram β-cells. (*A*) Proinsulin-to-insulin ratio determined by ELISA; $n = 6$ for each of two independent experiments. (*B–F*) Quantification of components of the UPR displayed as fold change compared with vehicle-treated control cells (set to 1). Western blot analysis and quantification for (*B*) nuclear ATF6α ($n = 3$) and (*C*) phosphorylated eIF2α ($n = 3$) in β-cells. (*D–F*) Quantitative PCR for mRNA levels of sXBP-1, ATF4 in β-cells, and GRP78 in iPS cells ($n = 3$ for each experiment). *$P < 0.05$. (*G*) Transmission electron microscope image showing ER morphology in control and Wolfram cells after 12-h treatment with 10 nmol/L TG. Arrows point to the ER. Scale bar, 500 nm. β-Cells were treated with TG 10 nmol/L for 12 h, and 1 mmol/L 4PBA or 1 mmol/L TUDCA was added 1 h prior to and during TG treatment. 4PBA 7d refers to treatment from day 9 to day 15 of β-cell differentiation.

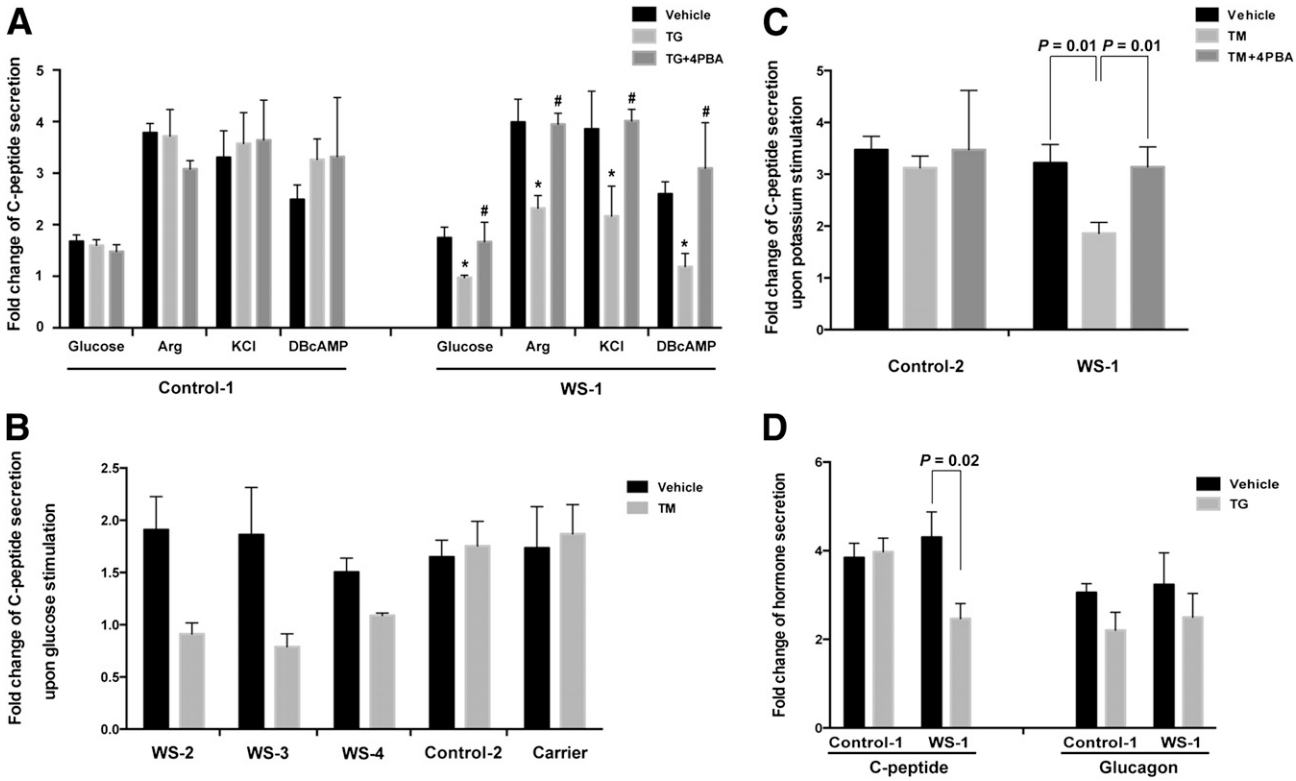

Figure 4—Differential effect of ER stress on insulin secretion in Wolfram and control cells. (*A*) Fold change of human C-peptide secretion in response to indicated secretagogues. Cells were incubated in 5.6 mmol/L glucose for 1 h followed by 16.9 mmol/L glucose, 15 mmol/L arginine, 30 mmol/L potassium, or 1 mmol/L DBcAMP + 16.9 mmol/L glucose for an additional hour. Fold change of human C-peptide secretion was calculated as the ratio of C-peptide concentration occurring in secretagogue-stimulated media over the concentration in 5.6 mmol/L glucose. Results represent three independent experiments, with $n = 3$ for each experiment. *$P < 0.05$ of TG vs. vehicle; #$P < 0.05$ of TG + 4PBA vs. TG. (*B*) Fold change of human C-peptide secretion to 16.9 mmol/L glucose stimulation; $n = 3$ for each of two independent experiments. (*C*) Fold change of human C-peptide secretion in response to 30 mmol/L potassium stimulation upon TM treatment. Results represent three independent experiments, with $n = 3$ for each experiment. (*D*) Fold change of human C-peptide and glucagon in control and Wolfram cells under indicated conditions; $n = 3$ for each of three independent experiments. Arg, arginine.

stress. When TG-treated cells were exposed to high ambient glucose (16.9 mmol/L), Wolfram cells failed to increase C-peptide secretion, while control β-cells increased C-peptide output by 1.6-fold (vs. 5.6 mmol/L glucose). Incubation with 4PBA prevented the effect of TG on Wolfram β-cells (Fig. 4*A*, Supplementary Fig. 6). The reduction in stimulated C-peptide secretion by TG was seen with all secretagogues tested. Independent of the secretagogues applied, the chemical chaperone 4PBA prevented the decrease in C-peptide secretion upon application of ER stressor (Fig. 4*A*). A reduction in stimulated C-peptide secretion was observed for β-cells generated from all four Wolfram subjects but not for the *WFS1* mutation carrier or the nonmutant control iPS cell line (Fig. 4*B* and *C*, Supplementary Fig. 7). The reduced β-cell function was not specific to TG: a comparable reduction in insulin secretion was also observed in TM-treated Wolfram β-cells upon potassium or glucose stimulation (Fig. 4*B* and *C*). Importantly, a wild-type *WFS1* transgene reduced sensitivity to the ER stress agent TG, showing a response to both arginine and DBcAMP stimulation comparable to controls (Supplementary Fig. 8).

To determine if the reduction in insulin secretion was due to β-cell death, we quantified the number of insulin-positive cells over 72 h, with or without TG treatment. Insulin cell number remained constant after 72 h incubation with 10nM TG (Supplementary Fig. 9*A*). We further tested the ER-stress-related cell death marker gene expression, such as CHOP (C/EBP homologous protein, also known as DNA damage-inducible transcript 3 encoded by the *DDIT3* gene) (34) and TXNIP (thioredoxin-interacting protein) (35), both proteins involved in ER-stress-dependent apoptosis. A higher increase of CHOP mRNA expression was observed in Wolfram cells compared with control cells after TG treatment for 12 h, but expression level of TXNIP mRNA showed no significant changes in control and Wolfram cells (Supplementary Fig. 9*B* and *C*). Therefore, ER stress did not reduce insulin secretion by inducing cell death during the time frame studied but rather by affecting the ability of β-cells to secrete insulin.

Because of the specific expression of WFS1 in β-cells (Fig. 1*D*) but not in glucagon-expressing cells, we anticipated that *WFS1* mutations differentially affect β- and α-cell function. We differentiated Wolfram cells into clusters containing both glucagon- and insulin-expressing cells (Fig. 1*D*) and stimulated these cells with arginine. As arginine stimulates both endocrine cell types, we were able to assess stimulated hormone secretion in the same cell cluster in the presence and absence of TG. TG treatment reduced arginine-stimulated glucagon secretion in control and *WFS1* mutant cells by 28 and 24%, respectively. In contrast, a reduction of stimulated insulin secretion occurred only in *WFS1* mutant cells (3% increase in control cells vs. 43% decrease in *WFS1* cells) (Fig. 4*D*). These results show that the insulin secretion phenotypes in *WFS1* mutant cells are not due to changes in glucagon release in adjacent cells (36) and demonstrate that WFS1 (which is not expressed in islet α-cells) specifically protects β-cells from the detrimental effects of ER stress.

Impaired Response to Glucose of Wolfram β-Cells In Vivo

In vitro studies may not fully recapitulate all relevant molecular cellular circumstances in a systemic physiological environment. The transplantation of β-cells allows testing functionality of β-cells in vivo over a time period of several months. After 12 days of in vitro differentiation, cell culture containing 70–80% PDX1+ cells, were transplanted under the kidney capsule of immunedeficient mice. Human C-peptide was detected 13 weeks post-transplantation in the serum of 13/16 mice transplanted with control cells and 14/20 mice transplanted with Wolfram cells. Basal C-peptide serum levels were comparable for both Wolfram and control HUES42-derived cells (Supplementary Fig. 10*A*). Human C-peptide was graft derived, as human C-peptide became undetectable in blood 2 days after the removal of the kidney containing the transplanted cells (Supplementary Fig. 10*B*). Cells contained in the graft coexpressed C-peptide and urocortin 3, which labels functional mature β-cells (37) (Fig. 5*A*). Upon systemic glucose challenge, Wolfram-derived cells were able to respond to glucose administered intraperitoneally by increasing human C-peptide secretion. However, they displayed significantly reduced responsiveness compared with human islets and β-cells derived from control stem cells (Fig. 5*B*). We then performed repeated measurement of human C-peptide over a 1-month period, starting from 3 months post-transplantation surgery when the mice were found to show glucose-stimulated human insulin secretion. During this 1-month period, human islets and control grafts remained unchanged in both fasting and glucose-stimulated C-peptide secretion. In contrast, both fasting C-peptide level and glucose responsiveness of Wolfram β-cells further decreased (Fig. 5*C* and *D*). To determine the level of ER stress in the transplanted cells, we isolated the grafts and performed immunohistochemistry for ATF6α and CHOP. Both ATF6α and CHOP staining were more intense in Wolfram β-cells, while control β-cells, human islets, as well as the surrounding grafted cells and mouse tissue showed lower intensity of staining (Fig. 5*E* and *F*). To test whether ER stress can mediate decreased C-peptide secretion from Wolfram β-cells in vivo, we challenged transplanted mice with TG. Basal C-peptide secretion from Wolfram cells was significantly decreased, while secretion of C-peptide from human islets remained constant (Supplementary Fig. 10*C* and *D*).

DISCUSSION

Here we report the first human cell model of an ER-related disorder, a stem-cell-based model of Wolfram syndrome. This model allowed us to study the consequences of ER stress on β-cell function. β-Cells of Wolfram subjects produce less insulin and have increased activity of three major UPR pathways, including PERK, IRE1, and ATF6. Addition of the chemical chaperone 4PBA reduced levels of UPR signaling pathway molecules and increased insulin content. These results demonstrate that WFS1 protects β-cells from protein folding stress and ER dysfunction, acting upstream of UPR signaling and not by regulating the activity of a particular component of the UPR pathway. Interestingly, low levels of UPR signaling affected insulin content but did not affect insulin processing or stimulated insulin secretion in vitro. However, following imposition of chemical ER stress, insulin processing, ER morphology, and stimulated insulin secretion were greatly affected. These phenotypes observed in vitro were recapitulated in vivo after cell transplantation: Wolfram-derived cells displayed significantly reduced responsiveness to increased circulating glucose, and the levels of immunohistochemical staining of ER-stress-associated protein ATF6α and CHOP were increased in Wolfram implants in comparison with controls, consistent with previous observations in a rodent model (12). Graft function of Wolfram but not control cells decreased over the time frame of 1 month, suggesting that Wolfram cells have a reduced ability to cope with a challenging metabolic environment in vivo, characterized by fluxes of glucose, free fatty acids, and other metabolites. Disease progression in human subjects may follow a similar course, from elevated UPR signaling resulting in reduced insulin content to chronic ER stress and β-cell failure. Our data suggest that unresolved ER stress will ultimately lead to ER dysfunction, reduced processing of insulin, and blunted insulin secretion.

In type 1 diabetes, a decreasing number of β-cells endeavor to meet metabolic demand for insulin, and in most instances of type 2 diabetes, the demand for insulin is increased because of peripheral insulin resistance. β-Cells of type 2 diabetes and type 1 diabetes subjects may possess greater intrinsic ability to increase insulin synthesis in response to metabolic demand than Wolfram β-cells but eventually encounter a similar situation, where metabolic demand requires insulin production at

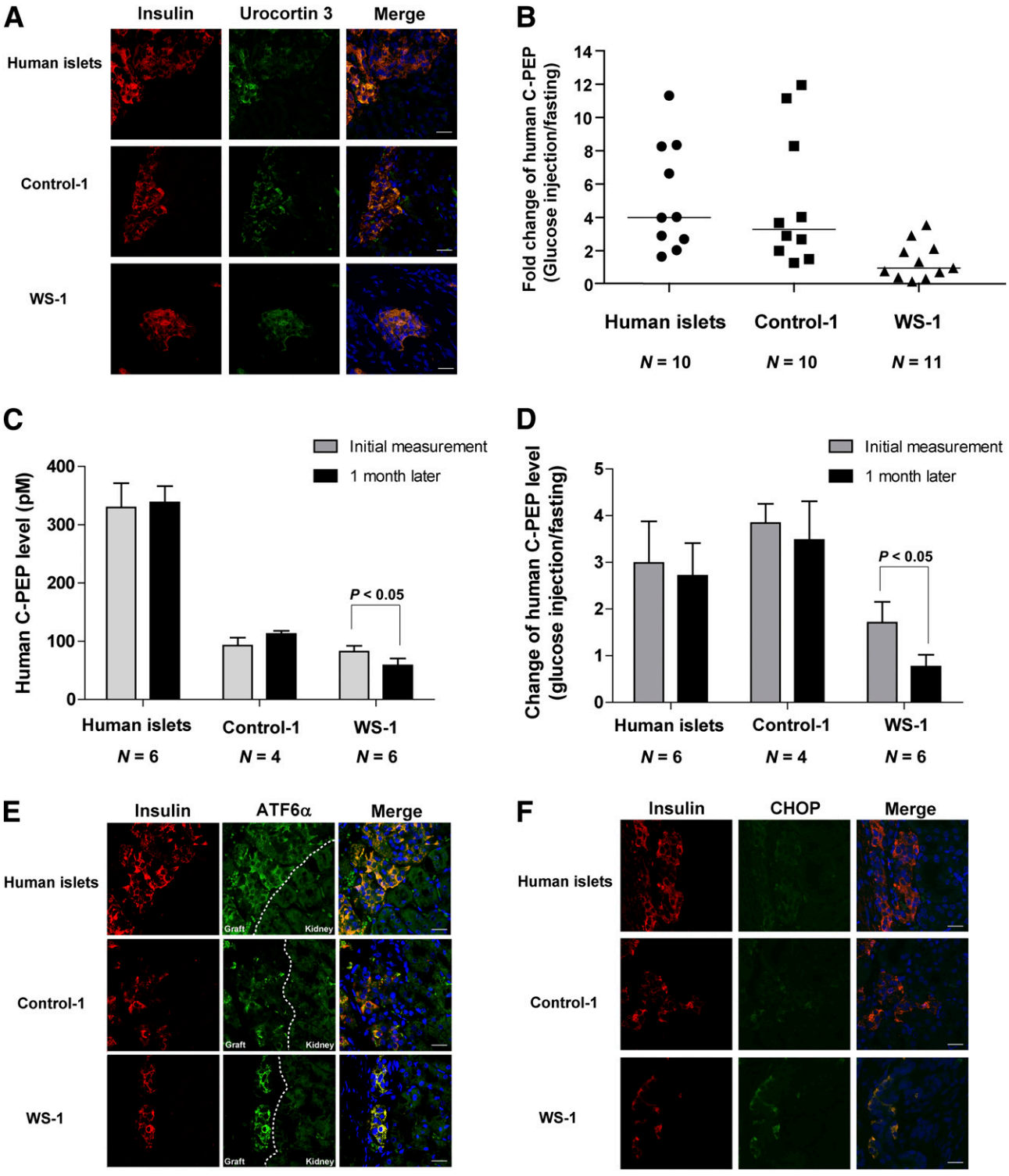

Figure 5—ER stress and reduced glucose-stimulated insulin secretion of Wolfram cells in vivo. (*A*) Immunohistochemistry for insulin and urocortin 3 in transplants. Scale bar, 20 μm. (*B*) Fold change of human C-peptide in the sera of mice transplanted with human islets and control and Wolfram cells after intraperitoneal glucose injection. Bars show the median. (*C*) Human C-peptide levels in the sera of transplanted mice over a 1-month time period. Error bars show SD. (*D*) Fold change of human C-peptide in the sera of transplanted mice over a 1-month time period. Error bars show SD. Immunohistochemistry for insulin and (*E*) ATF6α and (*F*) CHOP in transplants. Scale bar, 20 μm. C-PEP, C-peptide.

levels inducing a UPR response. If the disparity between demand and production remains unresolved, β-cell demise ensues. Increased expression of ER stress mediators has been observed in the islets of type 1 diabetic mice (38) and humans (39). Activation of ER-stress-associated genes (i.e., PERK and GRP78) has also been observed in the livers of mouse models of type 2 diabetes (40), and ER stress also appears to contribute to β-cell apoptosis in type 2 diabetes patients (41). Reducing the demand for insulin by intensive insulin therapy improves endogenous β-cell function in type 1 diabetes (42), and improving insulin sensitivity by peroxisome proliferator-activated receptor γ inhibitors or by weight loss meliorates type 2 diabetes, in part, because β-cell function is improved (43,44). In the aggregate, these earlier studies and those reported here support a role for ER stress in mediating aspects of the susceptibility and response of β-cells to failure in the context of diabetes.

Common alleles of *WFS1* are associated with increased diabetes risk (45), suggesting that our model of β-cell failure in Wolfram syndrome is also relevant to other forms of diabetes. Significantly, our model provides a platform for drug discovery and testing. We found that the chemical chaperone 4PBA is effective at reverting ER-stress-associated phenotypes in β-cells. In addition to insulin therapy, this molecule—or compounds with similar activity—may be useful in preventing or delaying β-cell dysfunction in Wolfram syndrome and possibly other forms of diabetes.

Acknowledgments. The authors are grateful to the research subjects who enabled this research. The authors thank Ellen Greenberg (Naomi Berrie Diabetes Center, Columbia University) for assistance with subject recruitment and study coordination, Kristy Brown (Department of Pathology and Cell Biology, Columbia University) for electron microscope study assistance, and Fumihiko Urano (Washington University School of Medicine) for providing the WFS1 antibody and for helpful discussions.

Funding. This work was supported by the New York Stem Cell Foundation, the Leona M. and Harry B. Helmsley Charitable Trust, the Berrie Foundation Program in Cellular Therapies of Diabetes, the National Institutes of Health (DK-52431, P30-DK-063608), and the Hunter Eastman Scholar Award in Translational Diabetes Research. D.E. is a New York Stem Cell Foundation–Robertson Investigator.

Duality of Interest. No potential conflicts of interest relevant to this article were reported.

Author Contributions. L.S. wrote the manuscript, researched data, and designed research. H.H. researched data, contributed to discussion, and designed research. K.F., H.M., K.W., M.Z., D.J.K., M.F., W.C., and C.L. researched data and contributed to discussion. R.G. reviewed and edited the manuscript. R.L.L. and D.E. reviewed and edited the manuscript and designed research. D.E. is the guarantor of this work and, as such, had full access to all the data in the study and takes responsibility for the integrity of the data and the accuracy of the data analysis.

References

1. Inoue H, Tanizawa Y, Wasson J, et al. A gene encoding a transmembrane protein is mutated in patients with diabetes mellitus and optic atrophy (Wolfram syndrome). Nat Genet 1998;20:143–148
2. Barrett TG, Bundey SE. Wolfram (DIDMOAD) syndrome. J Med Genet 1997; 34:838–841
3. Karasik A, O'Hara C, Srikanta S, et al. Genetically programmed selective islet beta-cell loss in diabetic subjects with Wolfram's syndrome. Diabetes Care 1989;12:135–138
4. Riggs AC, Bernal-Mizrachi E, Ohsugi M, et al. Mice conditionally lacking the Wolfram gene in pancreatic islet beta cells exhibit diabetes as a result of enhanced endoplasmic reticulum stress and apoptosis. Diabetologia 2005; 48:2313–2321
5. Ishihara H, Takeda S, Tamura A, et al. Disruption of the WFS1 gene in mice causes progressive beta-cell loss and impaired stimulus-secretion coupling in insulin secretion. Hum Mol Genet 2004;13:1159–1170
6. Hatanaka M, Tanabe K, Yanai A, et al. Wolfram syndrome 1 gene (WFS1) product localizes to secretory granules and determines granule acidification in pancreatic beta-cells. Hum Mol Genet 2011;20:1274–1284
7. Takeda K, Inoue H, Tanizawa Y, et al. WFS1 (Wolfram syndrome 1) gene product: predominant subcellular localization to endoplasmic reticulum in cultured cells and neuronal expression in rat brain. Hum Mol Genet 2001; 10:477–484
8. Takei D, Ishihara H, Yamaguchi S, et al. WFS1 protein modulates the free Ca(2+) concentration in the endoplasmic reticulum. FEBS Lett 2006;580: 5635–5640
9. Yurimoto S, Hatano N, Tsuchiya M, et al. Identification and characterization of wolframin, the product of the wolfram syndrome gene (WFS1), as a novel calmodulin-binding protein. Biochemistry 2009;48:3946–3955
10. Fonseca SG, Urano F, Weir GC, Gromada J, Burcin M. Wolfram syndrome 1 and adenylyl cyclase 8 interact at the plasma membrane to regulate insulin production and secretion. Nat Cell Biol 2012;14:1105–1112
11. Fonseca SG, Fukuma M, Lipson KL, et al. WFS1 is a novel component of the unfolded protein response and maintains homeostasis of the endoplasmic reticulum in pancreatic beta-cells. J Biol Chem 2005;280:39609–39615
12. Fonseca SG, Ishigaki S, Oslowski CM, et al. Wolfram syndrome 1 gene negatively regulates ER stress signaling in rodent and human cells. J Clin Invest 2010;120:744–755
13. Fusaki N, Ban H, Nishiyama A, Saeki K, Hasegawa M. Efficient induction of transgene-free human pluripotent stem cells using a vector based on Sendai virus, an RNA virus that does not integrate into the host genome. Proc Jpn Acad, Ser B, Phys Biol Sci 2009;85:348–362
14. Takahashi K, Tanabe K, Ohnuki M, et al. Induction of pluripotent stem cells from adult human fibroblasts by defined factors. Cell 2007;131:861–872
15. Hua H, Shang L, Martinez H, et al. iPSC-derived β cells model diabetes due to glucokinase deficiency. J Clin Invest 2013;123:3146–3153
16. Lee JH, Won SM, Suh J, et al. Induction of the unfolded protein response and cell death pathway in Alzheimer's disease, but not in aged Tg2576 mice. Exp Mol Med 2010;42:386–394
17. Merquiol E, Uzi D, Mueller T, et al. HCV causes chronic endoplasmic reticulum stress leading to adaptation and interference with the unfolded protein response. PLoS ONE 2011;6:e24660
18. Lu J, Wang Q, Huang L, et al. Palmitate causes endoplasmic reticulum stress and apoptosis in human mesenchymal stem cells: prevention by AMPK activator. Endocrinology 2012;153:5275–5284
19. Szot GL, Koudria P, Bluestone JA. Transplantation of pancreatic islets into the kidney capsule of diabetic mice. J Vis Exp 2007;9:404
20. Colosimo A, Guida V, Rigoli L, et al. Molecular detection of novel WFS1 mutations in patients with Wolfram syndrome by a DHPLC-based assay. Hum Mutat 2003;21:622–629

21. Chen AE, Egli D, Niakan K, et al. Optimal timing of inner cell mass isolation increases the efficiency of human embryonic stem cell derivation and allows generation of sibling cell lines. Cell Stem Cell 2009;4: 103–106
22. Hetz C. The unfolded protein response: controlling cell fate decisions under ER stress and beyond. Nat Rev Mol Cell Biol 2012;13:89–102
23. Lipson KL, Fonseca SG, Ishigaki S, et al. Regulation of insulin biosynthesis in pancreatic beta cells by an endoplasmic reticulum-resident protein kinase IRE1. Cell Metab 2006;4:245–254
24. Wong WL, Brostrom MA, Kuznetsov G, Gmitter-Yellen D, Brostrom CO. Inhibition of protein synthesis and early protein processing by thapsigargin in cultured cells. Biochem J 1993;289:71–79
25. Kozutsumi Y, Segal M, Normington K, Gething MJ, Sambrook J. The presence of malfolded proteins in the endoplasmic reticulum signals the induction of glucose-regulated proteins. Nature 1988;332:462–464
26. Ma Y, Hendershot LM. ER chaperone functions during normal and stress conditions. J Chem Neuroanat 2004;28:51–65
27. Yam GH, Gaplovska-Kysela K, Zuber C, Roth J. Sodium 4-phenylbutyrate acts as a chemical chaperone on misfolded myocilin to rescue cells from endoplasmic reticulum stress and apoptosis. Invest Ophthalmol Vis Sci 2007;48:1683–1690
28. de Almeida SF, Picarote G, Fleming JV, Carmo-Fonseca M, Azevedo JE, de Sousa M. Chemical chaperones reduce endoplasmic reticulum stress and prevent mutant HFE aggregate formation. J Biol Chem 2007;282:27905–27912
29. Berger E, Haller D. Structure-function analysis of the tertiary bile acid TUDCA for the resolution of endoplasmic reticulum stress in intestinal epithelial cells. Biochem Biophys Res Commun 2011;409:610–615
30. Ashcroft SJ. Glucoreceptor mechanisms and the control of insulin release and biosynthesis. Diabetologia 1980;18:5–15
31. Herchuelz A, Lebrun P, Boschero AC, Malaisse WJ. Mechanism of arginine-stimulated Ca2+ influx into pancreatic B cell. Am J Physiol 1984;246:E38–E43
32. Furman B, Ong WK, Pyne NJ. Cyclic AMP signaling in pancreatic islets. Adv Exp Med Biol 2010;654:281–304
33. Matthews EK, Shotton PA. Efflux of 86Rb from rat and mouse pancreatic islets: the role of membrane depolarization. Br J Pharmacol 1984;83:831–839
34. Oyadomari S, Mori M. Roles of CHOP/GADD153 in endoplasmic reticulum stress. Cell Death Differ 2004;11:381–389
35. Oslowski CM, Hara T, O'Sullivan-Murphy B, et al. Thioredoxin-interacting protein mediates ER stress-induced β cell death through initiation of the inflammasome. Cell Metab 2012;16:265–273
36. Bertuzzi F, Berra C, Socci C, Davalli AM, Pozza G, Pontiroli AE. Insulin and glucagon release of human islets in vitro: effects of chronic exposure to glucagon. J Endocrinol 1997;152:239–243
37. Blum B, Hrvatin SS, Schuetz C, Bonal C, Rezania A, Melton DA. Functional beta-cell maturation is marked by an increased glucose threshold and by expression of urocortin 3. Nat Biotechnol 2012;30:261–264
38. Tersey SA, Nishiki Y, Templin AT, et al. Islet β-cell endoplasmic reticulum stress precedes the onset of type 1 diabetes in the nonobese diabetic mouse model. Diabetes 2012;61:818–827
39. Marhfour I, Lopez XM, Lefkaditis D, et al. Expression of endoplasmic reticulum stress markers in the islets of patients with type 1 diabetes. Diabetologia 2012;55:2417–2420
40. Ozcan U, Cao Q, Yilmaz E, et al. Endoplasmic reticulum stress links obesity, insulin action, and type 2 diabetes. Science 2004;306:457–461
41. Laybutt DR, Preston AM, Akerfeldt MC, et al. Endoplasmic reticulum stress contributes to beta cell apoptosis in type 2 diabetes. Diabetologia 2007;50: 752–763
42. Shah SC, Malone JI, Simpson NE. A randomized trial of intensive insulin therapy in newly diagnosed insulin-dependent diabetes mellitus. N Engl J Med 1989;320:550–554
43. Gastaldelli A, Ferrannini E, Miyazaki Y, Matsuda M, Mari A, DeFronzo RA. Thiazolidinediones improve beta-cell function in type 2 diabetic patients. Am J Physiol Endocrinol Metab 2007;292:E871–E883
44. Dixon JB, Dixon AF, O'Brien PE. Improvements in insulin sensitivity and beta-cell function (HOMA) with weight loss in the severely obese. Homeostatic model assessment. Diabet Med 2003;20:127–134
45. Sandhu MS, Weedon MN, Fawcett KA, et al. Common variants in WFS1 confer risk of type 2 diabetes. Nat Genet 2007;39:951–953